Chemical Engineering Journal 164 (2010) 305–315

Contents lists available at ScienceDirect

Chemical Engineering Journal

journal homepage: www.elsevier.com/locate/cej

Effect of impeller speed on mechanical and dissolution properties of high-shear granules

C. Mangwandi[a], M.J. Adams[b], M.J. Hounslow[a], A.D. Salman[a,*]

[a] Particle Products Group, Department of Chemical and Process Engineering, The University of Sheffield, Mappin Street, Sheffield S1 3JD, UK
[b] Centre of Formulation Studies, University of Birmingham, Birmingham, UK

ARTICLE INFO

Article history:
Received 1 September 2009
Received in revised form 17 May 2010
Accepted 20 May 2010

Keywords:
Impeller speed
Granules
Packing
Strength

ABSTRACT

Impeller speed is one of the most crucial process variables that affect the properties of the granules produced in a high-shear granulator. Several reports can be found in literature that discuss the influence of impeller speed on the granules size. For instance some researchers like Knight report an increase of granule size with impeller speed [1,2], while others (Scheaefer et al. and Ramaker et al.) observed a decrease of granules size with increasing impeller speed [3,4]. However there is limited work reported in literature on the effect of the impeller speed on the mechanical properties of granules. Mechanical properties are important as they affect the performance of the granules on the other downstream process such as transportation and handling. The work reported here serves to address the missing in knowledge gap regarding the influence of impeller speed on mechanical properties granules. How the granulation system responds to the changes in the impeller speeds depends on binder that is used in the process. For this reason the two extreme cases, of a low viscosity binder system and high viscosity binder system are considered in this research. For low viscosity binder system it was observed that the granule size decreased with increasing impeller speed whilst for the high viscosity binder system the opposite was observed by Knight [1]. The granule strength, the Young's modulus and yield strength of the high viscosity granules increased with increasing impeller speed where as the opposite trends were observed for the low viscosity binder granules.

1. Introduction

High-shear granulators incorporate an impeller in the base and a vertically mounted chopper that operates at much greater speeds. The impeller provides the mechanical energy required for mixing the feed powder and the chopper is intended to break up granules that are formed. The effect of the impeller and chopper speed therefore depends on the response of the granules to this energy input. If an increase in impact energy results in more deformation of the granules, both the granule size and growth rate increase according to Knight [1] and Kokubo and Sunada [5]. At a sufficiently large energy, granule breakage will dominate and an increase in the impeller speed causes a decrease in granule size as has been observed previously (Schæfer et al. [6], Ramaker et al. [4]).

The influence of the energy input on granule growth was investigated by Knight [1]. Batches were produced at three impellor speeds (*viz*. 450, 800 and 1500 rpm) and it was found that the mean granule diameter increased with increasing mixer energy at 450 and 800 rpm. The mixing energy was varied by varying the mixing time at constant impeller speed and constant chopper speed. However, at an impeller speed of 1500 rpm, the effect of the energy input was less pronounced. They argued that growth was limited by an increased granule breakage. Schaefer et al. [7] reported that the impeller speed did not significant influence the intra-granular porosity. Hamdani et al. [8] employed a melt binder (Compritol 888) and observed a rapid increase in the mean granule size by almost a factor of six when the impeller speed was increased from 400 to 800 rpm. However a further increase in the impeller speed to 1000 rpm resulted in over-wetting of the system due to excessive melting of the binder. It was also found that a narrower granule size distribution resulted at greater impeller speeds.

Kinget and Kemel [9] found that increasing the chopper speed mainly improves the homogeneity of the granulation due to the absence of fines. No clarification was given on what they meant by homogeneity but probably they were referring to the breadth of the granule size distribution. In contrast, using similar materials, Schaefer et al. [7] found that at large chopper speeds the mean granule size was slightly reduced; there was no significant effect on the intra-granular porosity or the granule size distribution. Knight [1] found that the chopper assisted in narrowing the granule size distribution although the chopper was not used for the first 10 min of granulation.

* Corresponding author. Tel.: +44 0114 222 7560.
E-mail address: A.d.salman@sheffield.ac.uk (A.D. Salman).

1385-8947/$ – see front matter © 2010 Published by Elsevier B.V.
doi:10.1016/j.cej.2010.05.039

Nomenclature

a	parameter in equation Eq. (3) (–)
A	cross-sectional area (mm^2)
b	parameter in equation Eq. (3) (–)
C_t	packing coefficient (–)
D	diameter (mm)
E	granule's Young's modulus (Pa)
E^*	effective Young's modulus of the granules and platen system (Pa)
f	number density fraction (–)
F_l	compression force at failure point (N)
F	compression force (N)
h_0	initial bed height (mm)
$h_{0.5}$	bed height at a pressure of 0.5 MPa (mm)
m	wet mass (kg)
$\bar{m}_{in}$	mean mass of active ingredient in the sample (mg)
P	pressure (Pa)
R	granule radius (mm)
S	perimeter (mm)
V_s	volume (ml)
Y	fraction of active ingredient dissolved (–)

Greek letters

Δ	total displacement (mm)
Φ	circularity (–)
α	pressure coefficient (–)
χ	conductivity at time t ($\mu S\,cm^{-1}$)
χ_o	initial conductivity ($\mu S\,cm^{-1}$)
χ_∞	maximum conductivity ($\mu S\,cm^{-1}$)
ε_n	natural strain (–)
η	coefficient of variation (–)
τ	granule strength parameter (MPa)
υ_g	granule's Poisson's ratio (–)

Thies and Kleinebudde [10] investigated the effect of process variables on the growth rate, size and shape of sodium valproate pellets using glycerol monostearate as a meltable binder. They showed that impeller speed and binder concentration were the main variables influencing the mean size and size distribution. When both parameters were increased there was accelerated growth and high impeller speeds also improved the spheronisation of the pellets. In later work, they showed that there was mutual compensation between the binder content and the impeller speed *viz*. the size of the granules could be controlled by careful selection of the impeller speed and binder concentration [11]. Moreover, granules of the same average size obtained by appropriate selection of the impeller speed and the granulation time. Contrary to earlier studies, Ohno et al. [12], reported that the impeller speed had no significant effect on the mean size; the amount of water added and the granulation time had a greater influence.

The effect of impeller speed granule properties other than size has also been reported in literature [12–14]. Dévay et al. [13] used experimental design to investigate the effect of impeller speed and binder flow rate on the dissolution properties of granules produced from a mixture of lactose, Avicel and theophylline. The mean dissolution time, which was defined as the time taken to dissolve about 63% of the granules (by mass), was determined from the dissolution profiles and results showed that this parameter increases with increasing impeller speed up to a critical value and then decreases. The peak in the mean dissolution time was obtained at an impeller speed of 750 rpm. Ohno et al. [12] obtained dissolution profiles of granules produced from a multi-component mixture of lactose, hydroxypropyl cellulose and micro-crystalline cellulose (MCC) at different impeller speeds. Dissolution decreased when the impeller speed was increased. Mercury porosimetry was used to determine the pore size distribution and the median pore diameter of the granules decreased with increasing impeller speed. In a related work by Gabbott [14] the mean pore fraction of calcium carbonate and polyethylene glycol (PEG1500) granules was shown to decrease with increasing impeller speed.

Benali et al. [15] recently investigated the effect of impeller speed on the porosity and friability of multi-crystalline cellulose granules produced in a high-shear granulator with water as the binder. Increasing the impeller speed from 40 to 300 rpm resulted in a significant reduction in the granule porosity from about 60% to about 12%. However, no significant change in the granule porosity was observed when the speed was further increased to 400 rpm. The friability of the dry granules, which is a measure of strength, decreased from 60% to 2% when the impeller speed was increased from 40 to 150 rpm, indicating that the granules become stronger as the impeller speed is increased.

In the current paper, a systematic study the influence of impeller speed on the mechanical properties of granules is presented. Since the binder viscosity also affects the response of granules, two extreme cases were considered i.e. relatively weak and strong systems based on low and high viscosity binders. The granule strength, Young's modulus and yield strength of the granule were measured as a function of impeller speed.

2. Materials and methods

2.1. Preparation of binder

The low and high viscosity binders were distilled water and aqueous hydroxypropyl cellulose respectively. The HPC binder was prepared at room temperature as an 8% w/w solution in distilled water. This involved intensive mixing of the solution with a mechanical mixer for a period of 24 h. The rheological properties of the HPC solution were measured using a Rheomat RM180 rheometer (Maple Instruments Ltd., Canada). It was found to be Newtonian with a viscosity of about 150 mPa s.

2.2. Production of granules

The solid granules were prepared in a 10 L high-shear granulator (Romaco Roto Junior). The feed powder was a mixture of lactose monohydrate (Granulac 230, Molkerel Meggle GmbH, Germany) and potato starch (Solani, Pharma, Quality Avebe) with median sizes, d_{50}, of 33 and 44 μm, respectively. The particle size distributions of the powders were determined by laser diffraction using a Malvern Mastersizer (Malvern Instruments, UK) and the results are shown in Fig. 1. In all experiments, the starch to lactose ratio was 0.16 by weight and the binder to solid ratio was 0.125. The total mass of powder for each batch was 2500 g. The powder feed was pre-mixed for 2 min at an impellor speed of 250 rpm for all experiments. The binder was added for 1 min using the pour-in method and granulation was allowed to proceed for 6 min. Batches of granules were produced at different granulation speed ranging from 150 to 650 rpm. In all experiments a chopper was not used.

2.3. Drying and sieving

The granules were dried using the procedure previously described [16]. After drying each sub-sample was then passed through a Camsizer (Retsch GmbH, Germany) to measure the granule size distribution. The mass weighted mean, $x_{4,3}$ was calculated

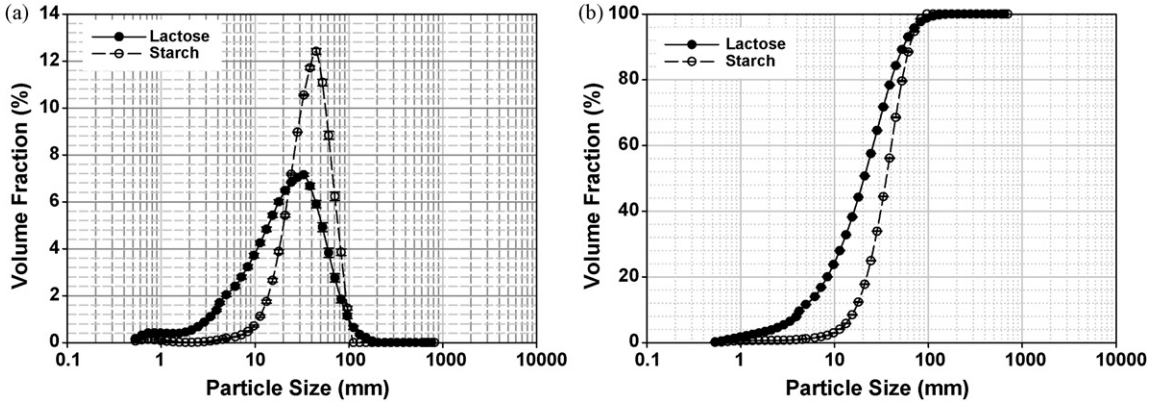

Fig. 1. Particle size distribution of the lactose and starch powder determined for laser diffraction using Malvern Mastersizer. Each plot is an average of five repetitions.

according to:

$$x_{4,3} = \frac{\mu_4}{\mu_3} = \frac{\int_0^\infty l^4 n(l)\,dl}{\int_0^\infty l^3 n(l)\,dl} \tag{1}$$

where $n\leftrightarrows(l)$ is the number based distribution; μ_3 and μ_4 are the 3rd and 4th moments, respectively. Granules in the size range 1.0–1.18 mm were selected for mechanical and flow analyses.

2.4. Granule shape and surface structure analysis

The granule circularity was used a shape parameter. The granule circularity was determined from images recorded using a stereo microscope using the same procedure described in Mangwandi et al. [16]. The circularity, ϕ, of the granules was determined from [17]:(2)$\phi = \frac{4\pi A}{S^2}$

The circularity data was fitted to a Gaussian distribution:

$$f = ae^{(-0.5(\phi-\phi_{0.5}/b))} \tag{3}$$

where f is number density, $\phi_{0.5}$ is the median circularity and b is the standard deviation of the distribution.

For surface structure analysis, images of single granules from the different batches were taken using a Stereo microscope at magnification of times 40 to see detailed structure of the granule surface. A qualitative comparison of the surface structure was made from these images.

2.5. Measurement of the granule strength

2.5.1. Single granule diametric compression measurements

Single granule diametric compression measurements for the size range 1.0–1.18 mm were performed using a Zwick/Roell Z 0.5 materials testing machine with a PC for real time data logging and analysis as previously described [16,18–20].

Assuming that the granules are spherical, at small displacements the applied force F may be described by the Hertz equation [21], thus:

$$F = \frac{\sqrt{2}}{3} R^{1/2} E^* \Delta^{3/2} \tag{4}$$

where R is the radius of the granule, E^* is the effective Young's Modulus and Δ is the total displacement. It is reasonable to assume that the Young's modulus of the platens is much greater than that of the granules so that the effective modulus, E^*, can be simplified to:

$$E^* \frac{E_g}{1-\upsilon_g^2} \tag{5}$$

where E_g and υ_g are the Young's modulus and Poisson's ratio of the granule, respectively. For porous materials, the typical value for Poisson's ratio is taken to be 0.2 [22]. For strains greater than the elastic limit, the granules deform plastically. If the uniaxial yield stress is independent of the applied strain, the loading data will be linear in this region with a gradient or stiffness, k_p, given by the following expression (Johnson [21]):

$$F = k_p \Delta = c\pi R \sigma_y \Delta \tag{6}$$

where c is the constraint factor and σ_y is the uniaxial yield stress. The constraint factor is about 2.8 for full plastic deformation.

The elastic limit of the granules was determined using the method previous discussed by Mangwandi et al. [16] which involves determining the point of the force-displacement curve which gives the best fit to Eqs. (4) and (6) to the data.

The strength was determined from the failure loads using the following expression [23]:

$$\sigma = 0.7 \frac{F_l}{\pi R^2} \tag{7}$$

where F_l is the failure load. The energy that is required to initiate fracture, W_B, was estimated from the area under the force-displacement to the point of failure:

$$W_B = \frac{1}{\pi R^2} \int_0^{\Delta_{\max}} F\,d\Delta \tag{8}$$

where $\Delta_{\max}$ is the displacement at fracture. The integral in Eq. (8) was evaluated by calculating the area under the force-displacement curve using the trapezium method using a computer program written in Visual Basic 6.0 (Microsoft Cooperation).

2.5.2. Granule porosity

The apparent density of the granules in the size range 1.0–1.18 mm was determined using the liquid-displacement method similar to the one described in [24]. The average granule porosity was then determined for the apparent density and true density of the granules using;

$$\varepsilon_p = \left(1 - \frac{\rho_a}{\rho_t}\right) \tag{9}$$

where ρ_a is the apparent granule density, and ρ_t is the theoretical true density of the granules.

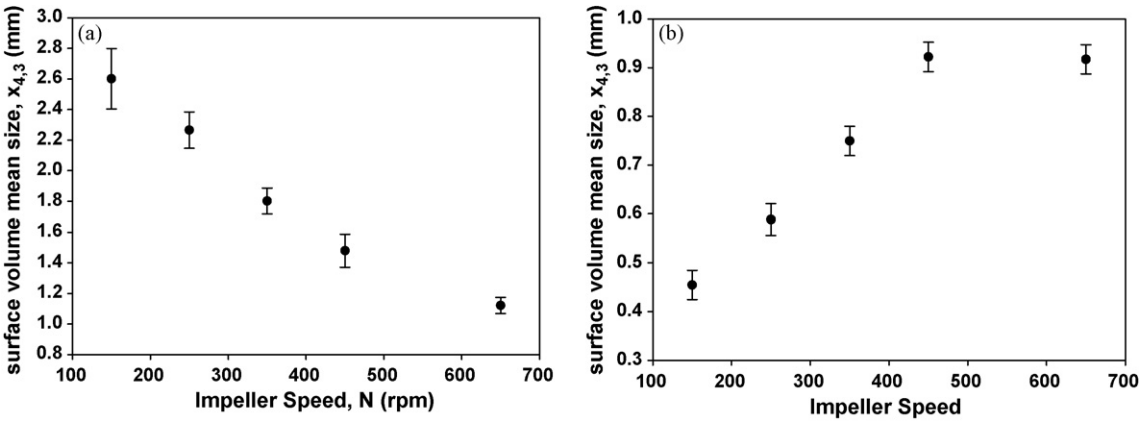

Fig. 2. Effect of impeller speed on average granule sizes. (a) Low viscosity system, (b) high viscosity system.

2.5.3. Confined uniaxial compression of multiple granules

For each sieve cut, ~350 mg granules were carefully weighed and poured into a steel cylindrical die with a diameter of 10 mm. The die was gently tapped to reduce packing irregularities. The granules were compressed at a speed of 5 mm/min to a maximum force of 450 N using the materials testing machine described previously. Ten repeat measurements were carried out for each condition. The die and punch were cleaned after each measurement to remove any dust or granules that had accumulated on the walls. The force-displacement data were analysed using a method described previously [25] to obtain the single granule strength:

$$\ln P = \ln\left(\frac{\tau}{\alpha}\right) + \alpha\varepsilon_n + \ln(1 - e^{(-\alpha\varepsilon_n)}) \quad (10)$$

where P is the applied pressure, ε_n is the natural strain, α is a pressure coefficient and τ is a measure of the single granule strength. The values of τ and α were obtained by fitting the data to Eq. (10) in the form $\ln P$ as a function of ε_n using non-linear regression.

2.5.4. Determination of packing coefficient and packing energy

The packing coefficient expresses the ability of particles or granules to rearrange at low compression pressures [26]. Values of <25% indicate a tendency to close pack under load whilst those in the ranges 25–30% and >30% indicate an intermediate and high resistance to pack. The packing coefficient is related to the flow characteristics with low values having a large flowability index according to Jenkine cell measurements [27]. Thus the packing coefficient can be used as a convenient procedure for assessing flow behaviour. In the current work the packing coefficient of the granules was determined from the data obtained by the confined compression [28]:

$$C_t = \left(\frac{h_0 - h_{0.5}}{h_0}\right) \times 100\% \quad (11)$$

where h_0 and $h_{0.5}$ are the initial bed height and that at a pressure of 0.5 MPa.

2.6. Dissolution measurements

Solutions of the non-functional active ingredient (Sodium Chloride, Analytical grade) in distilled water were prepared with different concentrations and the conductivities were measured at a temperature of 37 °C using a conductivity meter (Hanna 9000, Hanna Instruments, USA). This was repeated five times for each concentration to obtain a mean and standard deviation. A calibration of conductivity as a function of concentration was obtained on this basis. The dissolution of 100 mg granules in 250 ml distilled water was measured at the same temperature. The granules used in this test were in the size range 1.0 to 1.18 mm. This involved stirring with a paddle at 250 rpm and monitoring the conductivity of the solution as a function of time. The conductivity and temperature data were recorded automatically at 10 s intervals using a computer. Five repeat measurements were made.

The fraction of the active ingredient dissolved, Y, after a time, t, was determined as follows:

$$Y = \left(\frac{\chi - \chi_o}{\chi_\infty - \chi_o}\right) \times 100\% \quad (12)$$

where χ is the conductivity of the solution at a time t, and χ_o and χ_∞ are the initial and final conductivities. The Weibull distribution function was used to describe the data [13,29]:

$$Y = 1 - \exp\left(-\left(\frac{t - t_0}{\tau_d}\right)^{\beta}\right) \quad (13)$$

where τ_d is the time taken to dissolve 63.2% of the active ingredient, β is the shape factor and t_0 is the lag-time, which is zero in the current work.

2.7. Extent of mixing

The active ingredient content of 10 samples taken from granules in the size range 1.0–1.18 mm from each batch was measured. The mean of 10 measurements were determined for each batch, and the coefficient of variation of the active ingredient in the samples, η was determined as follows [16]:(14)$\eta = \frac{\bar{\sigma}}{\bar{m}_{in}}$ where $\bar{\sigma}$ is the standard deviation of active ingredient of the sample and $\bar{m}_{in}$ is the mean value.

3. Results

3.1. Granule size distribution

The effect of impeller speed on the mean granule size is shown in Fig. 2. For water as the binder, the mean size decreases with increasing impeller speed (Fig. 2(a), whereas they increase with the HPC binder (Fig. 2(b)).

3.2. Circularity

Fig. 3 shows the circularity distribution profiles in the size range 1.0–1.18 mm for the low viscous and high viscosity systems respectively; they are well described by a Gaussian function. The data were fitted using a non-linear regression analysis with R^2 values >0.99. For both systems the maximum circularity of the granules is obtained at an impeller speed of about 250 rpm (Fig. 4)

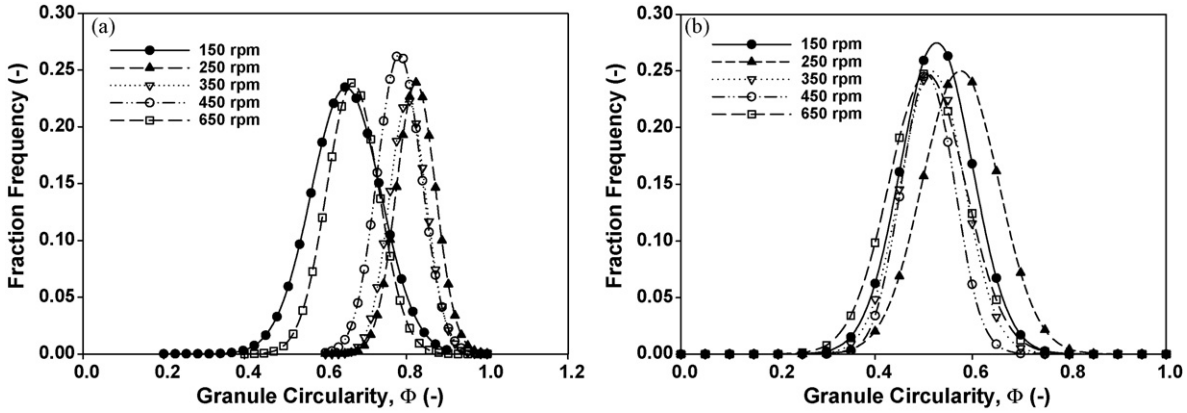

Fig. 3. Granule circularity profiles for granules in the size range 1.0–1.18 mm. (a) Low viscosity system, (b) high viscosity system. The lines in the graphs are non-linear regression fits to Eq. (3).

beyond which a marked reduction in the circularity with increasing impeller speed is observed. At any given impeller speed, water results in greater circularity compared with the HPC solution.

3.3. Granule porosity

The results depicted in Fig. 5 show the effect of impeller speed on the granule porosity. For water granules increasing the impeller speed from 150 to 250 rpm results in a reduction in the granule porosity from ~0.26 to ~0.25. A further increase in the impeller speed from 250 to 650 rpm results in an increase in the granule porosity to ~0.31. For the HPC granules a monotonic decrease in the granule porosity is observed as the impeller speed is increased.

3.4. Granule strength

A typical force-displacement curve for confined bed compression and the corresponding data fitted to Eq. (9) are shown in Fig. 6(a) and (b), respectively. The effect of the impeller speed on the strength parameters, τ for granules in the size range 1.0–1.18 mm are shown in Fig. 7. For water the strength increased from 0.16 to 0.22 MPa when the impeller speed is increased from 150 to 250 rpm then decreases to about 0.13 MPa when the speed is further increased to 650 rpm. Thus for the weak system in which granulating liquid is water, the graph can be divided into two regimes; one in which the increasing the impeller speed increases the strength, and another one where increasing the speed results in formation of weak granules. For the HPC binder; there is a monotonic increase from ~0.2 to about ~1 MPa when the impeller speed is increase between 150 and 650 rpm.

In the case of water as the binder; increasing the impeller speed results in an overall reduction in the granule failure load (see Fig. 8(a)). Each data point is the mean of at least 50 granules selected at random from the 1.0 to 1.18 mm sieve cut. The error bars represent the standard errors. Fig. 8 shows the corresponding effect of the impeller speed on the single granule strength. For the HPC granules, there is an increase from ~3.2 to ~7.0 MPa when the impeller speed is increased from 150 to 650 rpm. For water granules increasing the impeller speed from 250 to 650 rpm results in an overall reduction of strength from 0.7 to ~0.55 MPa.

The single granule strength parameters are about an order of magnitude greater than those obtained from the confined uniaxial compression measurements (Fig. 9). The corresponding values of the breakage energies from the diametric compression of single water granules decreased from ~0.075 to ~0.055 mJ/mm^2 when the impeller speed was increased from 250 to 650 rpm though there was an increase when impeller speed was increased from 150 to 250 rpm. This is not surprising considering that the porosity of the granules increased with increasing impeller speed in the same range of impeller speed. For the case of HPC granules, increasing the impeller speed in the same range results with an increase in breakage energy from ~0.05 to ~0.25 mJ/mm^2 (Fig. 9).

3.5. Yield stress and Young modulus

The variation of the Young's modulus and yield stress are shown in Figs. 10 and 11. For the HPC granules, the Young's

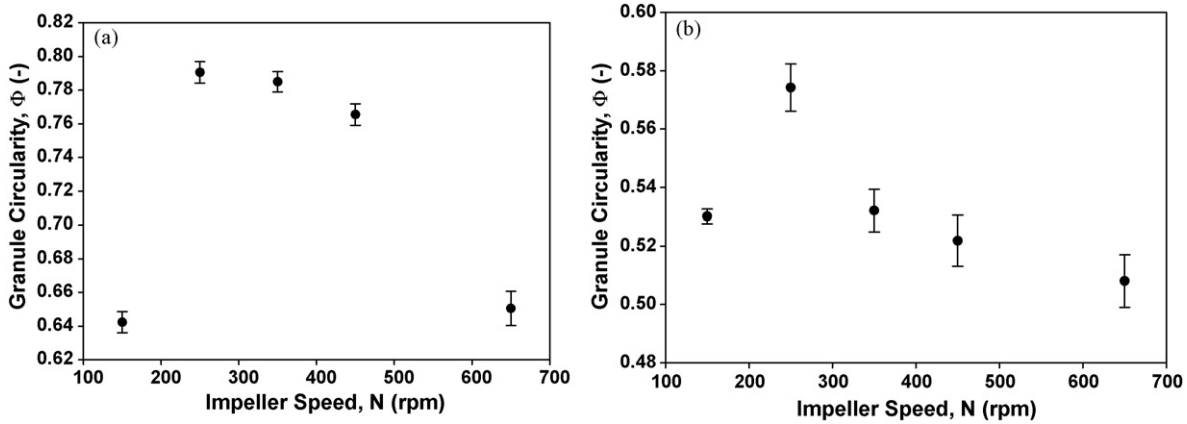

Fig. 4. Effect of impeller speed on average granule circularity. (a) Low viscosity system, (b) high viscosity system.

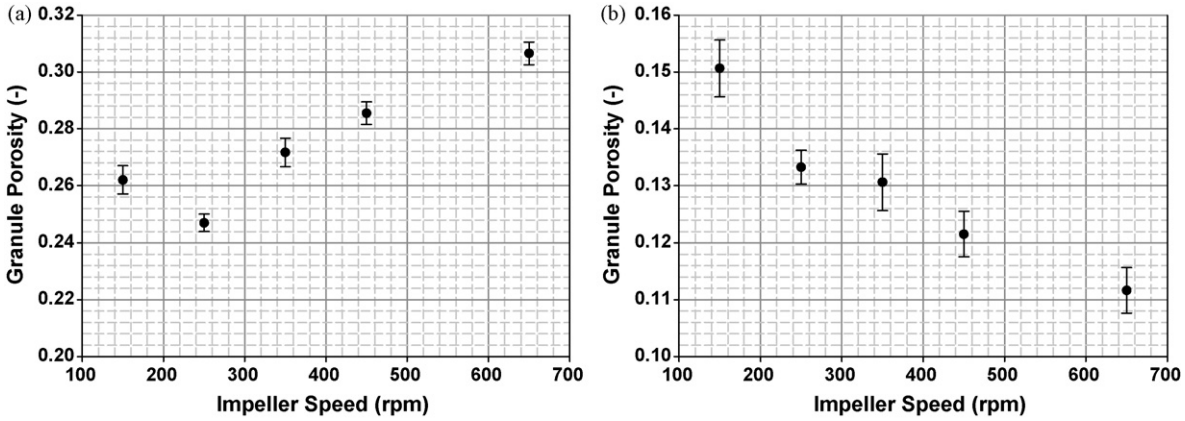

Fig. 5. Effect of impeller speed on granule porosity for granules in the size range 1.0–1.18 mm. (a) Low viscosity system, (b) high viscosity system.

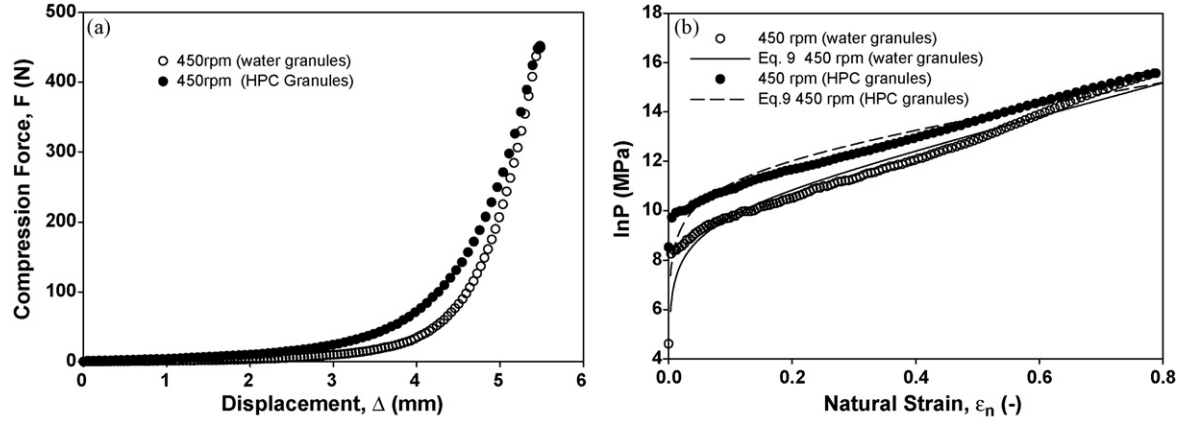

Fig. 6. Typical data for the confined uniaxial compression of granules obtained with different impeller speeds: (a) force-displacement profiles and (b) fits of the data to Eq. (9).

modulus increases from ~350 to ~460 MPa when the impeller speed was increased. The opposite trend was observed with water as the binder with the values decreasing from ~210 to ~170 MPa. There are similar trends for the yield stress (Fig. 11).

3.6. Variation of final bed height with impeller speed

The initial and final bed heights of the granules are shown in Table 1. It is quiet evident from this table that the for HPC granules there is a slight increase in the mass of the sample which is attributed to increase in the bulk density of the granules as the impeller speed is increased. The final bed height increased as the impeller speed was increased. Increasing the impeller speed leads to a reduction in the compressibility of the granules. For the water granules it can be noted that the final bed first increased (between 150 and 250 rpm) and the decreased with increasing impeller speed. This indicates that the compressibility of the granules decreases and then increases with increasing impeller speed.

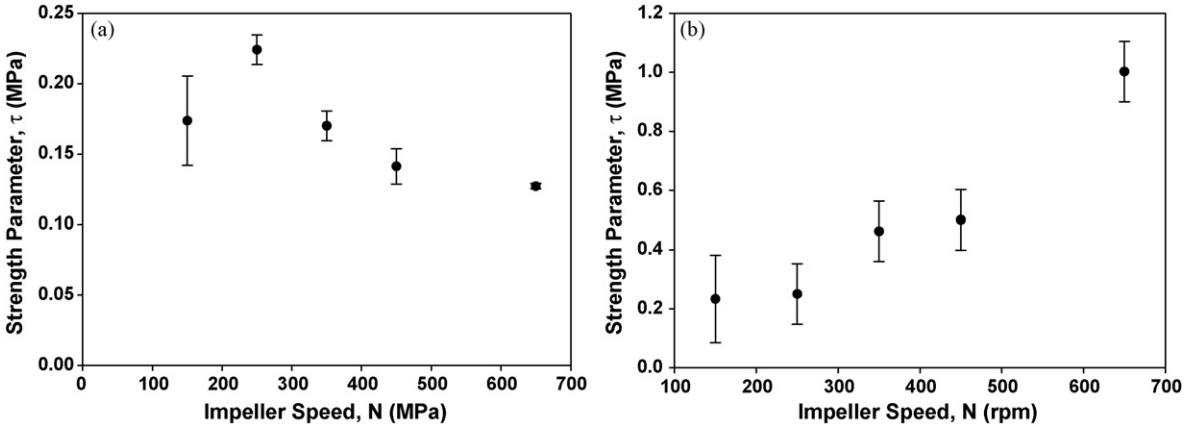

Fig. 7. Effect of impeller speed on the granule strength for granules in the size range 1.0–1.18 mm. (a) Low viscosity system, (b) high viscosity system.

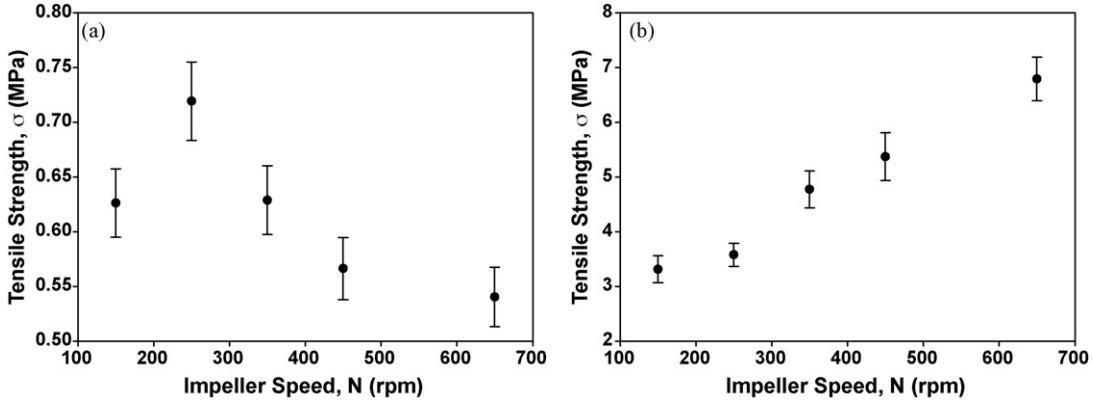

Fig. 8. Effect of impeller speed on the granule tensile strength of granules in the size range 1.0–1.18 mm. (a) Low viscosity system, (b) high viscosity system.

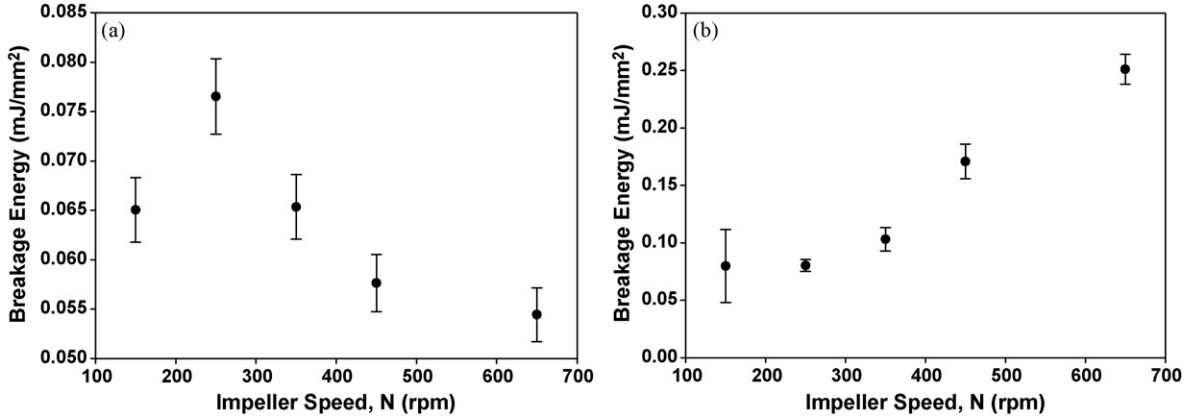

Fig. 9. Effect of impeller speed on the breakage energy for granules in the size range 1.0–1.18 mm. (a) Low viscosity system, (b) high viscosity system.

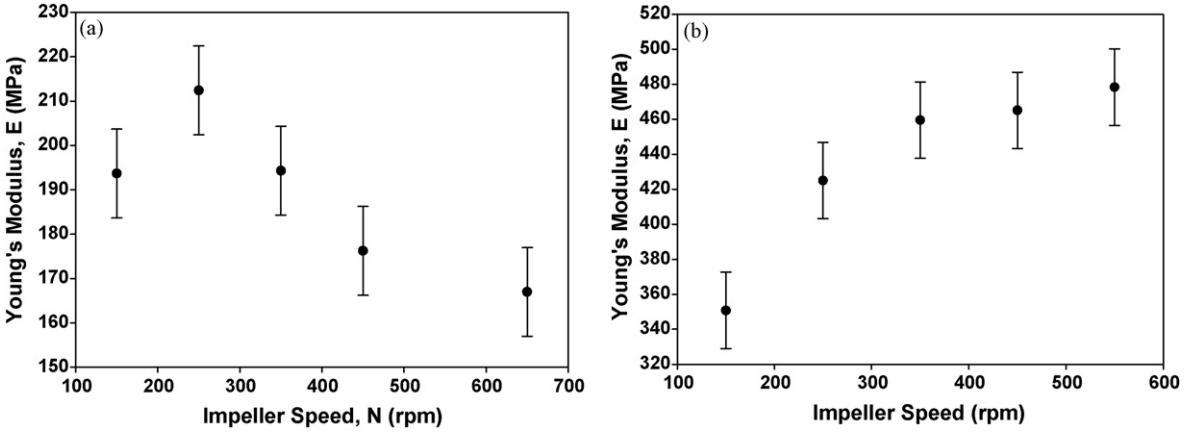

Fig. 10. Effect of impeller speed on the granule Young's Modulus of granules in the size range 1.0–1.18 mm. (a) Low viscosity system, (b) high viscosity system.

Table 1
Final bed height of samples during confined bed compression of granules.

Impeller speed (rpm)	Final bed height	
	Water granules mm (±0.02)[a]	HPC granules mm (±0.02)
150	4.39	4.20
250	4.59	4.32
350	4.57	4.51
450	4.52	4.57
650	4.18	4.64

All samples have the same bed height of 10 mm just before compression.
[a] Standard deviation of 10 measurements.

3.7. Packing properties

The effect of the fill factor on the packing properties of granules in the size range 1.0–1.18 mm is shown in Fig. 12. For water, the values suggest that the packing behaviour is poor since for all impeller speeds investigated $C_t > 30\%$ [26–28,30]. The packing coefficient increases from ~38% to ~43% with increasing impeller speed suggesting that the packing ability of the granules deteriorates with increasing impeller speed. For HPC granules in the same size range, the packing coefficient decreases almost linearly from ~40% to ~28% when the impeller speed is increased from 150 to 650 rpm, which suggest an improvement in the flow characteris-

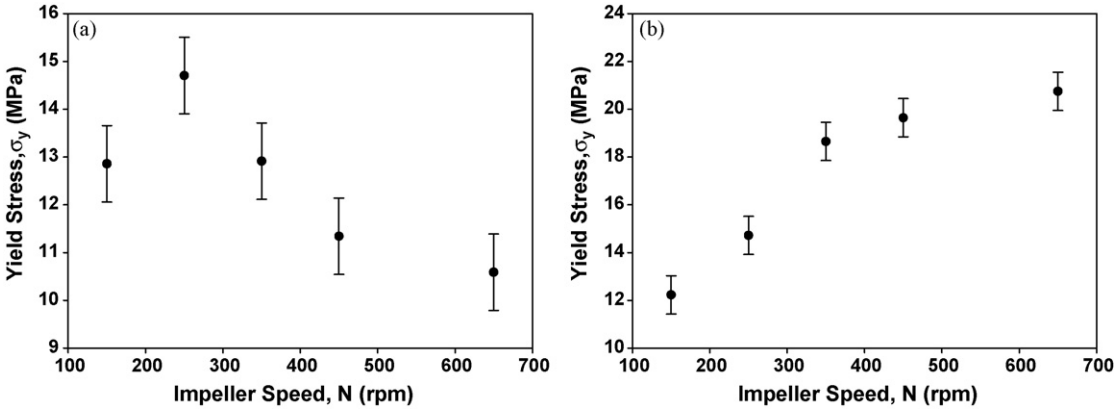

Fig. 11. Effect of impeller speed on the Yield Stress of granules in the size range 1.0 to 1.18 mm. (a) Low viscosity system, (b) high viscosity system.

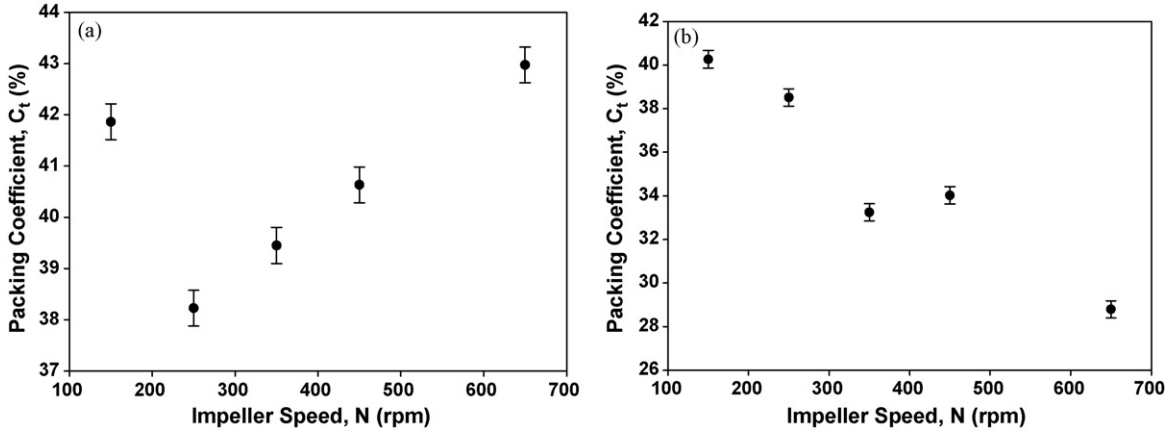

Fig. 12. Effect of impeller speed on the Packing coefficient for granules in the size range 1.0–1.18 mm. (a) Low viscosity system, (b) high viscosity system.

tics. Overall, the values were less than those with water at a given impeller speed. Thus the HPC binder provides improved packing properties compared with water.

The images shown in Fig. 13 show the difference in the surface structure of the HPC granules obtained at different impeller speed. It can be seen from these images that the surface smoothness of the granules increases with increasing impeller speed. This might explain why the packing of the HPC granules improves with increasing impeller speed.

Fig. 14 depicts the difference in the surface structure of water and HPC granules obtained at same impeller speed, 650 rpm. It shows that the HPC granules have smoother surfaces than the water granules this explains the differences in the packing that is exhibited by these two types of granules at different.

3.8. Dissolution properties

The rate of dissolution of the granules depends on both the experimental conditions during dissolution and the properties of the granules such as porosity and size of the granules. Since it has already been shown that the mechanical properties of the granules are influenced by the impeller speed used during granulation, it would be sensible to expect the granules to exhibit different dissolution rates. The dissolution profiles for water as the binder granules at different impeller speeds are

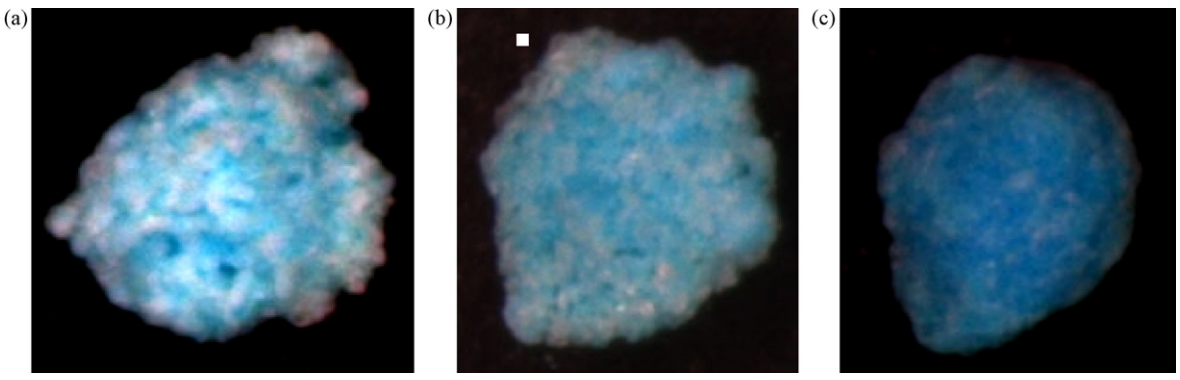

Fig. 13. Effect of impeller speed on surface properties of lactose starch HPC granules in the size range 1.0–1.18 mm. (a) 150 rpm), (b) 250 rpm, (c) 650 rpm. Images were taken using Stereo microscope.

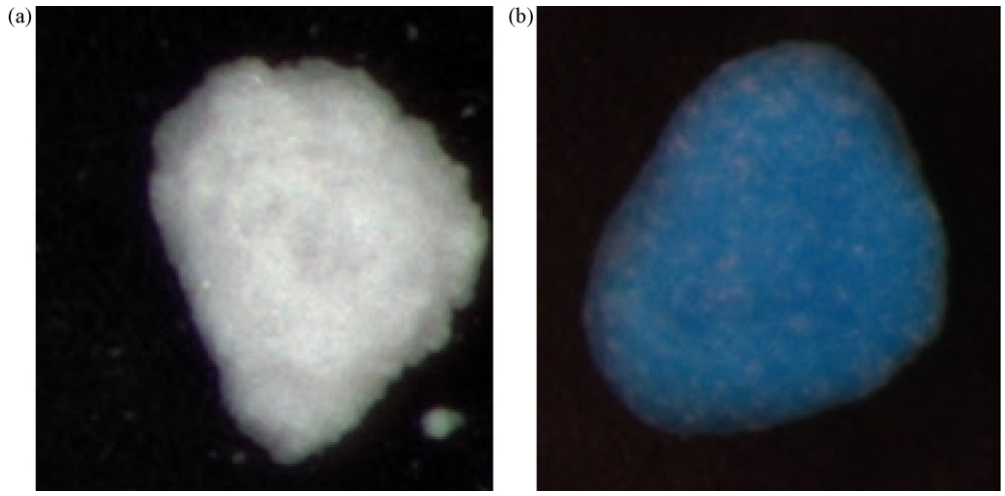

Fig. 14. Images showing the surface structure of different types of granules (a) low viscosity system, (b) high viscosity system produced at impeller speed of 650 rpm.

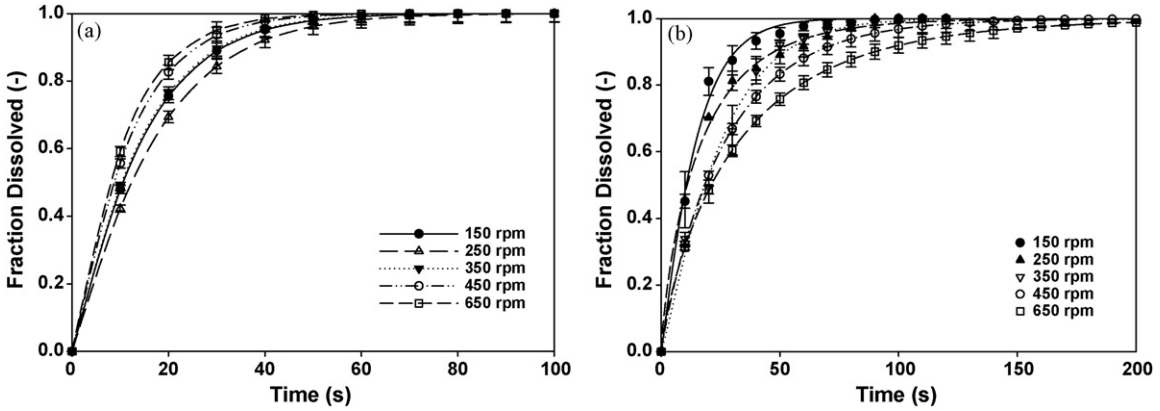

Fig. 15. Dissolution profiles for granules in the size range 1.0–1.18 mm. (a) Low viscosity system, (b) high viscosity system. The lines are fit to equation Eq. (12).

shown in Fig. 15(a) and (b). Each datum point is the mean of at least five repetitions and the error bars show the standard deviations. The dissolution time is relatively fast compared to the acquisition interval of 10 s but the differences appear to be statistically significant. The curves are the best fit to Eq. (12) for obtaining the mean dissolution time, τ_d, which decrease with increasing impeller speed except at the smallest speed (Fig. 16(a)). The opposite trend is found for the HPC granules (Fig. 16(b)).

The coefficient of variation of the active ingredient content in the granules is plotted as a function of impeller in Fig. 17. For the water granules the values decrease with increasing impeller speed from ~10% to ~1% in the range studied. This means that the quality of mixing improves with increasing impeller speed. A similar trend is observed for the HPC granules were the values are in the range ~20% to ~2% for the same range of impeller speed. The HPC values are obviously higher point the fact that mixing is better for the low viscosity system than for high viscosity system.

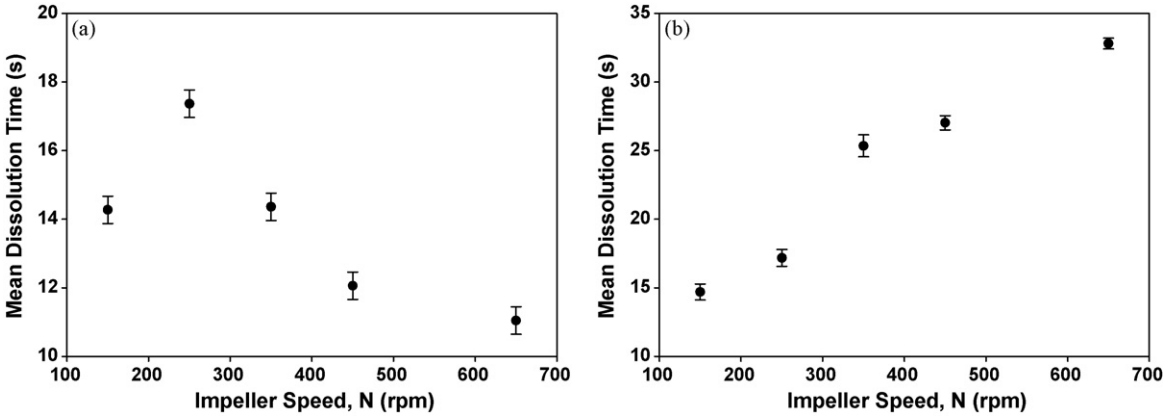

Fig. 16. Effect of impeller speed on Mean Dissolution time for granules in the size range 1.0–1.18 mm. (a) Low viscosity system, (b) high viscosity system.

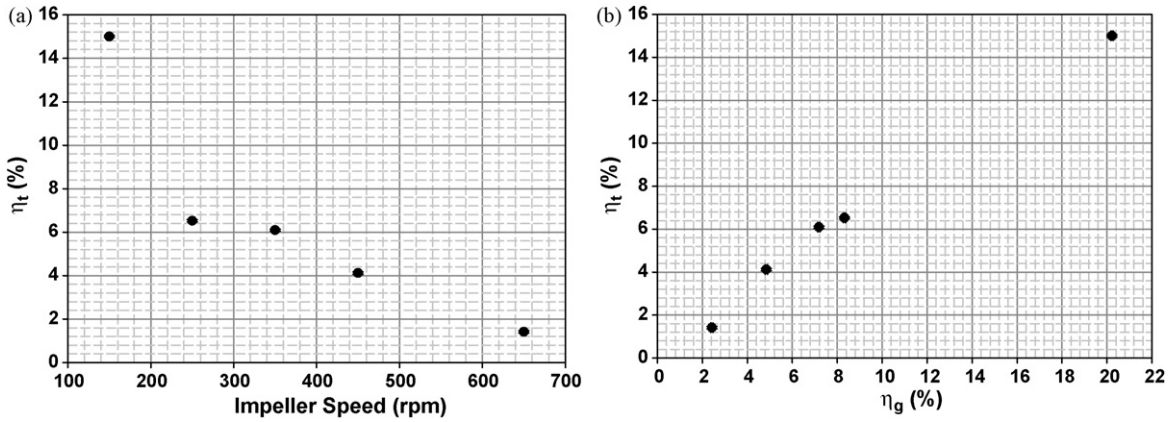

Fig. 17. Effect of impeller speed on the coefficient of variation of active ingredient in granules in the size range 1.0–1.18 mm. (a) Low viscosity system, (b) high viscosity system.

4. Discussion

It has been shown that binders with a low viscosity result in a crushing and layering growth mechanism while high viscosity binders result in a coalescence growth mechanism [31]. Thus the decrease in granule size with increasing impeller speed for granules with water as a binder may be reasonably attributed to an increase in breakage. For the granules with the HPC binder as the binder the increase in size may be ascribed to an increase in the number and kinetic energy of the collisions. This behaviour may be described in terms of the Stokes deformation number, which is the ratio of the impact energy to the dynamic strength of the granules and which has been used as criteria to predict whether a granule will break during an impact event [32–34]. For Newtonian fluids, both the normal and tangential components of the hydrodynamic forces between particles are proportional to the viscosity [35,36]; more complex expressions have been derived for power-law fluids [37,38]. The viscosity of the HPC binder (104 mPa s) is about 100 times greater than that of water. Thus if it is assumed to first order that the wet granule strength scales simply with the viscosity of the binder, the values corresponding to the HPC binder will be about two orders of magnitude greater than those with water as the binder. This difference is consistent with the growth mechanisms. However, the sizes associated with the HPC binder are less than for water. In the case of the coalescence mechanism, growth depends on the liquid binder being forced to the surface of the granules [39] and this is retarded at higher viscosities [31]. The current data on circularity are also consistent with these growth mechanisms as observed previously [31]. The circularities of the granules made with the HPC binder are less than those with the HPC binder because coalescence leads initially to dumbbell geometries. The values decrease with increasing speed because of the greater deformation of the granules.

The strength of the dried water granules was found to decrease with increasing impeller speed which is in contradiction to the results obtained by Benali et al. [15] who observed a decrease in the granule friability and porosity when the speed was increased. Since the porosity decreased it would be expected that the strength would increase with increasing impeller speed. A contributory factor could be that the binder was applied as a spray rather than poured as was the case in the current study. This influences the growth mechanism and hence the granule structure [40,41]. For the HPC granules, the increase in the strength with the impeller speed is consistent with the coalescence mechanism in which the porosity is reduced by impacts of increasing frequency and kinetic energy. The effect is clearly quite large given the factor of three increases in strength for the speed range considered. The mean values with water as a binder are almost an order of magnitude smaller than those with the HPC binder which is the expected trend for the addition of a water soluble polymer. There is a relatively small change in the strength and the values decrease with speed except for a small maximum at low speeds. This supports the contention that a different growth mechanism is operating in which the granules fracture rather than deform so that changes in porosity rely on layering existing granules as this may result in a relatively constant porosity.

Results obtained in this work also show that impeller speed also influences the packing properties of the granules. A high value of packing coefficient ($C_t > 30\%$) indicates poor packing behaviour whilst low values of packing coefficient indicate ($C_t < 25\%$) excellent packing and flow properties [28]. Values of packing coefficient between 25% and 30% point out to intermediate packing and flow behaviour. The results for packing coefficient of HPC granules show that increasing the impeller speed results in formation of granules that are easier to pack since the packing coefficient decreases with increasing impeller speed. The improvement of the parking ability of the HPC granules may be explained qualitatively in terms of change in the surface properties of the granule properties when the impeller is increased. Running the impeller speed higher speed promotes smoothening of the granules surface which facilitates granule flow and packing.

It has been shown that the impeller speed has an effect on the granule porosity and strength. It would be expected that the other granule characteristics like dissolution and compressibility would also be influenced by the impeller speed. A reduction in the granules porosity should result in reduced dissolution rate i.e. longer mean dissolution time. Results obtained in this work are a confirmation to this; for the HPC granules increasing the dissolution time results in increased mean dissolution time while a reduction in the mean dissolution time is observed for the water granules.

5. Conclusions

The impeller speed does not only affect the size distribution and the means granule size during high-shear granulation, but it also has an influence on the granules structure and shape which affect the end-use properties of the granules such as dissolution rate, compaction and survival during handling. The impeller speed is also thought to affect the quality of mixing of the different components of the formulation. However the effect of the impeller speed on the granule size also depends on the material variables like viscosity and surface tension of the binder used therefore careful consideration must be taken in process design to ensure that the products of the process will be of the required quality.

References

[1] P.C. Knight, An investigation of the kinetics of granulation using a high shear mixer, Powder Technology 77 (2) (1993) 159–169.
[2] P.C. Knight, A. Johansen, H.G. Kristensen, T. Schaefer, J.P.K. Seville, An investigation of the effects on agglomeration of changing the speed of a mechanical mixer, Powder Technology 110 (3) (2000) 204–209.
[3] T. Schaefer, B. Taagegaard, L.J. Thomsen, H. Gjelstrup Kristensen, Melt pelletization in a high shear mixer. IV. Effects of process variables in a laboratory scale mixer, European Journal of Pharmaceutical Sciences 1 (3) (1993) 125.
[4] J.S. Ramaker, M.A. Jelgersma, P. Vonk, N.W.F. Kossen, Scale-down of a high-shear pelletisation process: flow profile and growth kinetics, International Journal of Pharmaceutics 166 (1) (1998) 89–97.
[5] H. Sunada, M. Hasegawa, T. Makino, H. Sakamoto, K. Fujita, T. Tanino, H. Kokubo, T. Kawaguchi, Study of standard tablet formulation based on fluidized-bed granulation, Drug Development Industrial Pharmacy 24 (3) (1998) 225–233.
[6] T. Schæfer, P. Holm, H.G. Kristensen, Drug Dev, Melt granulation in a laboratory scale high shear mixer, Drug Development Industrial Pharmacy 16 (1990) 1249–1277.
[7] T. Schaefer, B. Taagegaard, L.J. Thomsen, H. Gjelstrup Kristensen, Melt pelletization in a high shear mixer. V. Effects of apparatus variables, European Journal of Pharmaceutical Sciences 1 (3) (1993) 133–141.
[8] J. Hamdani, A.J. Moës, K. Amighi, Development and evaluation of prolonged release pellets obtained by the melt pelletization process, International Journal of Pharmaceutics 245 (1–2) (2002) 167–177.
[9] R. Kinget, R. Kemel, Preparation and properties of granulates containing solid dispersions, Acta Pharmaceutica Technologica 31 (2) (1985) 57–62.
[10] R. Thies, P. Kleinebudde, Melt pelletisation of a hygroscopic drug in a high shear mixer: Part 1. Influence of process variables, International Journal of Pharmaceutics 188 (2) (1999) 131–143.
[11] R. Thies, P. Kleinebudde, Melt pelletisation of a hygroscopic drug in a high shear mixer: Part 2. Mutual compensation of influence variables, European Journal of Pharmaceutical Sciences 10 (2) (2000) 103–110.
[12] I. Ohno, S. Hasegawa, S. Yada, A. Kusai, K. Moribe, K. Yamamoto, Importance of evaluating the consolidation of granules manufactured by high shear mixer, International Journal of Pharmaceutics 338 (1–2) (2007) 79–86.
[13] A. Dévay, K. Mayer, S. Pál, I. Antal, Investigation on drug dissolution and particle characteristics of pellets related to manufacturing process variables of high-shear granulation, Journal of Biochemical and Biophysical Methods 69 (1–2) (2006) 197–205.
[14] I.P. Gabbott, Designer Granule: Beating the Trade Off Between Granule Strength and Dissolution Time, Department of Chemical and Process Engineering, The University of Sheffield, Sheffield, 2007, p. 181.
[15] M. Benali, V. Gerbaud, M. Hemati, Effect of operating conditions and physico-chemical properties on the wet granulation kinetics in high shear mixer, Powder Technology 190 (1–2) (2009) 160–169.
[16] C. Mangwandi, M.J. Adams, M.J. Hounslow, A.D. Salman, Effect of batch size on mechanical properties of granules in high shear granulation, in: 9th International Symposium on Agglomeration and 4th International Granulation Workshop, Sheffield, United Kingdom, 2009.
[17] J. Vertommen, P. Rombaut, R. Kinget, Shape and surface smoothness of pellets made in a rotary processor, International Journal of Pharmaceutics 146 (1) (1997) 21–29.
[18] Y.S. Cheong, M.J. Adams, A.F. Routh, M.J. Hounslow, A.D. Salman, The production of binderless granules and their mechanical characteristics, Chemical Engineering Science 60 (14) (2005) 4045–4053.
[19] C. Mangwandi, M.J. Adams, M.J. Hounslow, A.D. Salman, Evolution of the mechanical properties of granules in a high-shear granulation process, in: Particulate Systems Analysis 2008, Particle Characterisation Interest Group of the Royal Society of Chemistry, Stratford-upon-Avon, UK, 2008.
[20] C. Mangwandi, Y.S. Cheong, M.J. Adams, M.J. Hounslow, A.D. Salman, The coefficient of restitution of different representative types of granules, Chemical Engineering Science 62 (1–2) (2007) 437–450.
[21] K.L. Johnson, Contact Mechanics, Cambridge University Press, Cambridge, UK, 1985.
[22] B.S. Chun, H.S.H.-S. Lim, M. Sagong, K. Kim, Development of a hyperbolic constitutive model for expanded polystyrene (EPS) geofoam under triaxial compression tests, Geotextiles and Geomembranes 22 (4) (2004) 223–237.
[23] Y. Hiramatsu, Y. Oka, Determination of the tensile strength of rock by a compression test of an irregular test piece, International Journal of Rock Mechanics and Mining Society 3 (1966) 89–99.
[24] S.M. Iveson, J.D. Litster, B.J. Ennis, Fundamental studies of granule consolidation Part 1: Effects of binder content and binder viscosity, Powder Technology 88 (1) (1996) 15–20.
[25] M.J. Adams, M.A. Mullier, J.P.K. Seville, Agglomerate strength measurement using a uniaxial confined compression test, Powder Technology 78 (1) (1994) 5–13.
[26] F. Chantraine, M. Viana, S. Cazalbou, N. Brielles, O. Mondain-Monval, C. Pouget, P. Branlard, G. Rubinstenn, D. Chulia, From compressibility to structural investigation of sodium dodecyl sulphate—Part 2: a singular behavior under pressure, Powder Technology 177 (1) (2007) 41–50.
[27] M. Viana, C.M.D. Gabaude-Renou, C. Pontier, D. Chulia, The packing coefficient: a suitable parameter to assess the flow properties of powders, Kona 19 (2001) 89–93.
[28] C.M.D. Gabaude, J.C. Gautier, P. Saudemon, D. Chulia, Validation of a new pertinent packing coefficient to estimate flow properties of pharmaceutical powders at a very early development stage, by comparison with mercury intrusion and classical flowability methods, Journal of Materials Science 36 (2001) 1763–1773.
[29] F. Langenbucher, Parametric representation of dissolution–rate curves by the RRSBW distribution, Pharmazeutische Industrie 38 (1976) 472–477.
[30] C. Pontier, E. Champion, M. Viana, D. Chulia, D. Bernache-Assollant, Use of cycles of compression to characterize the behaviour of apatitic phosphate powders, Journal of the European Ceramic Society 22 (8) (2002) 1205.
[31] P.J.T. Mills, J.P.K. Seville, P.C. Knight, M.J. Adams, The effect of binder viscosity on particle agglomeration in a low shear mixer/agglomerator, Powder Technology 113 (1–2) (2000) 140.
[32] S.M. Iveson, P.A.L. Wauters, S. Forrest, J.D. Litster, G.M.H. Meesters, B. Scarlett, Growth regime map for liquid-bound granules: further development and experimental validation, Powder Technology 117 (1–2) (2001) 83.
[33] G.I. Tardos, M.I. Khan, P.R. Mort, Critical parameters and limiting conditions in binder granulation of fine powders, Powder Technology 94 (3) (1997) 245.
[34] K. van den Dries, O.M. de Vegt, V. Girard, H. Vromans, Granule breakage phenomena in a high shear mixer; influence of process and formulation variables and consequences on granule homogeneity, Powder Technology 133 (1–3) (2003) 228.
[35] N.A. Frankel, J. Schultz, On the viscosity of a concentrated suspension of solid spheres, Chemical Engineering Science 22 (1967) 847.
[36] A.J. Goldman, R.G. Cox, H. Brenner, Slow viscous motion of a sphere parallel to a plane wall-motion through a quiescent fluid, Chemical Engineering Science 22 (1967) 637.
[37] W. Huang, H. Li, Y. Xu, G. Lian, Hydrodynamic force between two hard spheres tangentially translating in a power law fluid, Journal of Non-Newtonian Fluid Mechanics 61 (2006) 1480–1488.
[38] G. Lian, Y. Xu, W. Huang, M.J. Adams, On the squeeze flow of a power-law fluid between rigid spheres, Journal of Non-Newtonian Fluid Mechanics 100 (2001) 151–164.
[39] S.M. Iveson, J.D. Litster, Growth regime map for liquid-bound granules, AIChE Journal 44 (7) (1998) 1510–1518.
[40] P. Holm, T. Schaefer, H.G. Kristensen, Granulation in high speed mixers. Part 1. Effects of process variables during kneading, Pharmaceutical Industry 46 (1983) 101–106.
[41] P.C. Knight, T. Instone, J.M.K. Pearson, M.J. Hounslow, An investigation into the kinetics of liquid distribution and growth in high shear mixer agglomeration, Powder Technology 97 (3) (1998) 246.